# Analyst

## Accepted Manuscript

This article can be cited before page numbers have been issued, to do this please use: R. Duan, Y. Li, Y. He, Y. Yuan and H. Li, *Analyst*, 2020, DOI: 10.1039/D0AN01187H.




ROYAL SOCIETY OF CHEMISTRY

rsc.li/analyst

View Article Online
DOI: 10.1039/D0AN01187H

ARTICLE

# Quantitative and sensitive detection of lipase using liquid crystal microfiber biosensor based on whispering-gallery mode

Received 00th January 20xx,
Accepted 00th January 20xx

DOI: 10.1039/x0xx00000x

Rui Duan,[ab] Yanzeng Li[c], Yichen He[a], Yonggui Yuan*[ab], and Hanyang Li*[ab]

In this study, we demonstrate a quantitative and sensitive strategy for monitoring lipase concentration using a liquid crystal (LC) microfiber biosensor based on whispering-gallery mode (WGM). LC 4-cyano-4'-pentylbiphenyl (5CB) microfiber was doped with glycerol trioleate (GT) and used as both an optical microcavity and a sensing element. The self-assembled monolayer of surfactant was formed at the LC/aqueous solution interface by the enzymatic reaction between lipases and GT, which resulted in the reorientation of the 5CB molecules from a planar to a homeotropic configuration. Interestingly, the structural change of 5CB microfiber can be sensitively captured by the WGMs and quantitatively characterized by the wavelength shift. With this method, lipase with concentrations as low as 0.01 μg/mL in aqueous solution can be detected within 200 seconds, which is lower than the optimal value based on LC materials reported so far. In addition, our biodetection system is highly selective for lipase. We believe that the proposed biosensor has a high potential for the detection of biochemical molecules.

## 1. Introduction

In the past decade, liquid crystal (LC) materials have great prospects in the application of biological assays and chemical sensors [1,2]. This is mainly attributed to the high optical sensitivity of LCs to their molecules' arrangement. Depending on the type of molecules anchoring to the LCs' interface, the strength exerted on the local LC molecules can be varying, which results in a change in the local LC molecules' arrangement and alters the optical response correspondingly.[1-5]. More complex interface interactions such as protein binding[6,7], enzymatic reaction [8], and DNA hybridization [9] have also been successfully monitored by LC interface sensors. At present, biosensors based on LC materials generally use the naked eye to judge and identify analytes with a polarized optical microscope (POM). However, this existing method of interpreting the sensor output is impractical, and the naked-eye-based readout method may have adverse impact on the testing accuracy and reliability.

We have suggested a whispering-gallery mode (WGM) based approach to effectively resolve the abovementioned difficulty in the biochemical detection. WGMs are optical eigenmodes in an optical microresonator with a geometrically symmetrical structure [10-13]. Light propagates inside the circular microcavity by means of total internal reflection at the cavity's boundaries, and only light waves oscillating in phase can form standing waves which are well-known as WGMs. Due to their high quality (Q) factor, WGM resonators are extremely sensitive to changes in their refractive index and their surrounding environment [14-17]. These changes can be captured by the WGM spectrum and quantitatively characterized by resonance frequency/wavelength shifts. Recently, WGM-based optical sensors have been widely studied for label-free detection of biological and chemical molecules including, viruses [18], proteins [19,20], and DNA [21,22]. Furthermore, WGM biosensors have ultra-high sensitivity and ultra-low detection limit, which has been confirmed by the successful detection of single molecules [23,24].

Lipases (EC 3.1.1.3) play an important role in lipid metabolism [25,26]. These enzymes are widely found in animals, plants, and microorganisms (such as molds and bacteria) [27,28]. Among them, lipases are abundant in the pancreas and adipose tissue of animals, which control the processes such as digestion, absorption, fat reconstruction, and lipoprotein metabolism. It is reported that the mean values of lipase in human sera are 12.3 ± 6.8 μg/L in adults and 4.5 ± 2.7 μg/L in newborns[29]. Normally, lipases can be removed from the plasma by filtration and metabolism in the renal tubules. However, high levels of active lipases can damage kidney cells, causing serious kidney disease and even organ failure. In addition, the transformation of cells from a normal state to a cancerous state is accompanied by changes in several metabolic pathways, one of which is an increase in the concentration of monoacylglycerol induced by lipases [30]. To date, several methods have been demonstrated to monitor the presence of lipases, including fluorescence detection,

[a] College of Physics and Optoelectronic Engineering, Harbin Engineering University, Harbin 150001, China. Email: yuanyonggui@aliyun.com; hanyang_li@qq.com
[b] Key Lab of In-fiber Integrated Optics, Ministry Education of China, Harbin Engineering University, Harbin 150001, China.
[c] James Franck Institute, University of Chicago, 929 East 57th Street, Chicago, Illinois 60637, United States.

View Article Online
DOI: 10.1039/D0AN01187H



colorimetric assays, and chromatographic procedures [31,32]. While these analytical techniques are of great significance for the detection of lipases, they also have own limitations. Since lipases are critical for sustaining life, it is

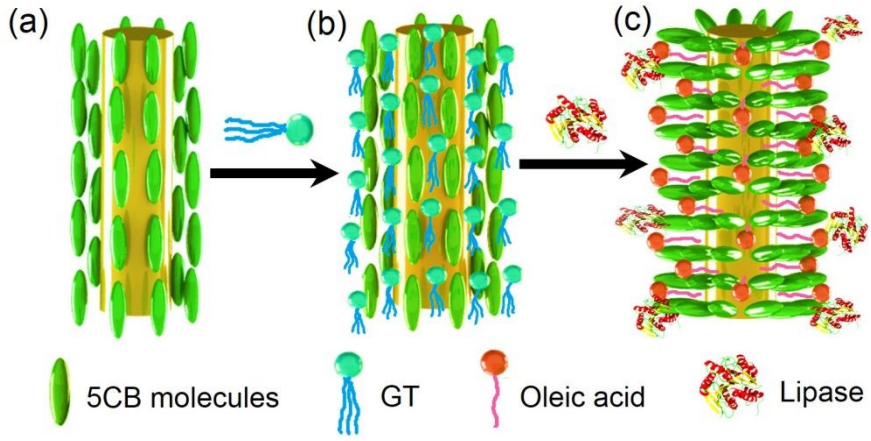


**Fig. 1.** Schematic representation of the orientation of LC 5CB molecules before and after the enzymatic reaction between lipase and GT: (a, b) planar orientation; (c) homeotropic orientation.

necessary to further develop higher sensitive and more reliable strategies for lipase detection.

In this study, we propose a novel LC microfiber biosensor based on WGM for real-time, quantitative, and sensitive monitoring of lipase concentration. Compared with the conventional spherical LC resonators, this LC microfiber resonator with cylindrical configuration has two obvious advantages. Firstly, the cylindrical resonator has a longitudinal degree of freedom up to several centimeters, while the spherical LC resonator does not have the longitudinal degree of freedom (Fig. S1). This makes the sensing range of cylindrical LC resonator greatly increased, and even has the potential of distributed detection of biochemical reactions. Secondly, the preparation process of such cylindrical microcavity is simpler compared to the spherical configuration, which allows for mass production without the involvement of complicated microfluidic control equipment. Considering these two advantageous aspects of the cylindrical resonators, 4-cyano-4′-pentylbiphenyl (5CB) microfibers were selected to serve as both optical microcavities and biosensing elements. The internal structural change of 5CB microfibers was sensitively captured and quantitatively characterized by WGMs. We showed that the wavelength shift of WGMs could be used as an effective indicator of lipase concentration and was more sensitive and accurate than the conventional LCs optical appearance detection method. A detection limit of 0.01 μg/mL lipase was achieved using our WGM-based 5CB microfiber biosensor and was lower than other known LC material-based lipase detection methods.

## 2. Experimental section

### 2.1 Materials

Nematic LC 4-cyano-4'-pentylbiphenyl (5CB), lipase (from porcine pancreas), orlistat (lipase inhibitor), urease, acetylcholinesterase (AChE), penicillinase, catalase were purchased from Sigma–Aldrich. Glycerol trioleate (GT, a substrate of lipase, 99%), polymethyl methacrylate (PMMA, average MW ~ 996000 g/mol), laser dye DCM, trichloromethane, sodium hydroxide obtained from Aladdin. All aqueous solutions were prepared with deionized (DI) water collected from a Milli-Q water purification system.

### 2.2 Preparation of functionalized microfiber lasers

The host materials for the microfiber lasers were 5CB and PMMA. PMMA was chosen due to its stability and transparency and could be used as internal medium to support for microlasers. GT (0.03 g) and DCM (0.01 g) acted as the functional material and laser dye of the microlaser, respectively, and were dissolved in 5CB (1 g). Subsequently, the mixed solution was ultrasonically treated for 40 min to ensure dispersibility and uniformity. Next, PMMA (0.5 g) was dissolved in 5 mL of trichloromethane and subjected to a half-hour ultrasonic treatment to obtain a transparent and homogeneous matrix solution. In order to obtain PMMA microfiber with a fixed diameter, a fiber probe was manufactured by using flame heating and stretching [33-35]. The diameter of the fiber probe is consistent with the diameter of the PMMA microfibers we want to obtain. Then the probe was dipped into the PMMA solution and withdrawn rapidly to fabricate PMMA microfibers. However, in the process of fiber drawing, due to the influence of gravity, only about one centimeter of fiber diameter in contact with the end face of the probe is highly uniform. Finally, the PMMA microfibers were immersed in the prepared 5CB samples for surface functionalization. The thickness of the LC layer is about 2 μm in 65 μm-diameter-LC microfibersused used in sensing experiments. The content of GT doped in the LC layer is 3 wt.%. In the sensing experiment, the length of the 5CB microfiber is about one centimeter. These functionalized microfibers were transferred to a phosphate buffered saline (PBS) solution and stored for future use. In order to avoid the influence of pH on the anchoring state of 5CB molecules, the

concentration of PBS we used is 0.05 M and the pH value is 7.0.

### 2.3 Changes in the internal structure of 5CB microfiber during the enzymatic reaction between lipase and GT

Enzymatic hydrolysis of lipases occurs at the oil/water interface layer[26,27] and allows for a unique advantage when using LCs materials for lipase detection. Lipase can catalyze the hydrolysis of GT (a substrate of lipase) to produce oleic acid at the LC/aqueous solution interface [36,37].

Normally, LCs are unable to self-assemble a monolayer at the interface spontaneously because of the hydrophobic nature of GT, and the LC molecules still adopt a planar alignment (Figs. 1a and 1b). However, when lipases are present in the aqueous solution, oleic acid is released by the enzymatic reaction between lipase and GT. Deprotonated oleic acid molecules can self-assemble at the LC/aqueous interface, inducing a change in the orientation of LC molecules from planar to homeotropic (Fig. 1c).

### 2.4 Measurement

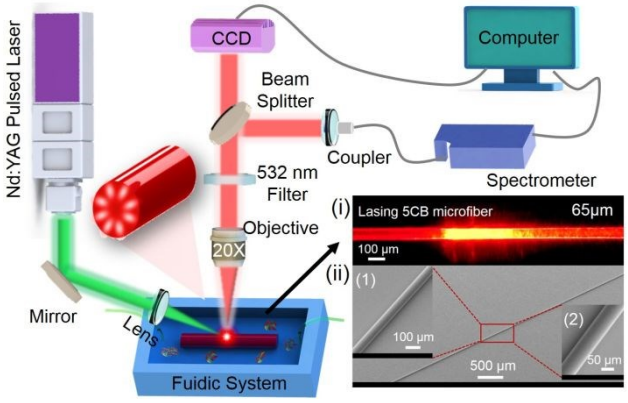


**Fig. 2.** Schematic diagram of the experimental setup. A micro-photoluminescence (μ-PL) system was used to investigate the optical properties of the individual 5CB microfiber laser. Inset: (i) The photoluminescence images of lasing 5CB microfiber with a diameter of 65 μm. (ii) Scanning electron micrograph (SEM) images of the preliminary microfibers. The fiber showed a smooth outer surface and good uniformity.

A micro-photoluminescence (μ-PL) system was used to investigate the optical properties of the individual 5CB microfiber lasers, as shown in Fig. 2. The pump light emitted from a Q-switched Nd: YAG laser (wavelength: 532 nm, repetition frequency: 10 Hz) was first focused by an optical lens. Then the dye-doped microfiber was excited by the focused free-space light. The PL signals were collected by a 20× objective and the pump light was blocked by a 532 nm filter. Next, the filtered light was delivered to the spectrometer with a spectral resolution of 0.05 nm (PG2000, Ideaoptics Technology, China) for data collection. The polarized optical microscope (BX41 P, Olympus, Japan) and a camera with a CCD (DP21, Olympus, Japan) were used to observe the optical appearance of 5CB microfibers.

## 3. Results and discussion

### 3.1 *WGM lasing spectra of 5CB microfiber*

One of the limiting factors hindering the development of WGM sensors comes from evanescent coupling-based optical coupling schemes that require a waveguide to physically connect the resonator to external devices such as relatively fragile tapered fibers or prisms. These coupling structures are mechanically unstable and difficult to combine with microfluidic system. In addition, a precise method is needed to adjust coupling gap between the waveguide and the microresonator on the nanometre scale to control the coupling efficiency, which makes the detection device overly complicated and fragile [38]. Therefore, in this study, we adopted an active resonator structure and the fluorescent dye DCM was used as the gain medium of the microcavity. Lasing spectra were collected by the free-space optical device, which created a simple, robust, and practical detection system.

Figure 3a plots the power-dependent μ-PL spectra of GT-doped 5CB microfiber with a diameter of 65 μm. Under relatively low pump pulse energy (PPE, < 0.89μJ), the PL spectrum is mainly determined by spontaneous emission. At PPE higher than the lasing threshold of 0.89 μJ, initial sharp peaks emerged from the broad emission. The lasing intensity increases sharply with the increase of PPE. In the illustration of Fig. 3a, an integrated PL intensity of the peaks with different

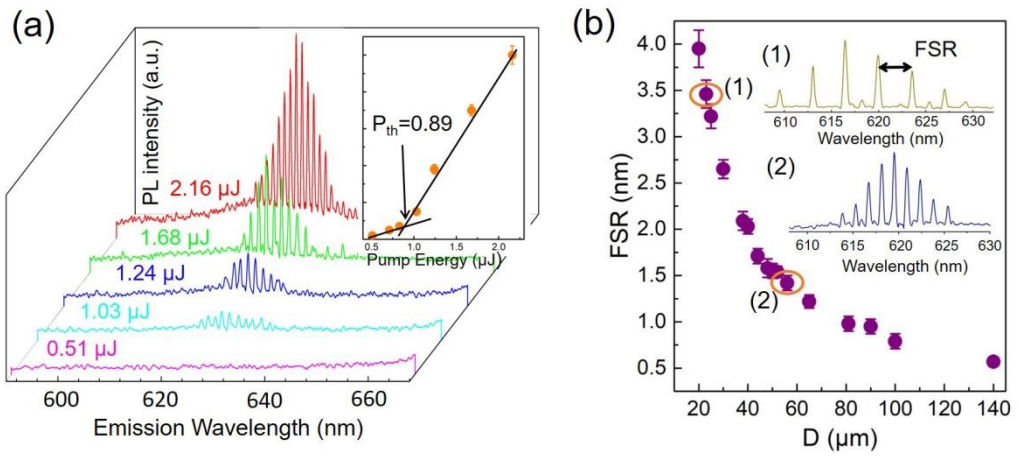

View Article Online
DOI: 10.1039/D0AN01207H

**Fig. 3.** (a) Pump power-dependent μ-PL spectra from GT-doped 5CB microfiber with a diameter of 65 μm. The inset shows the integrated PL intensity with pulse energy and the nonlinear increase similar to the knee joint shows the lasing phenomenon. (b) FSRs as a function of 5CB microfiber diameters. The insets show the WGM spectra of two typical microfibers with a diameter of (1) 33 and (2) 56 μm.

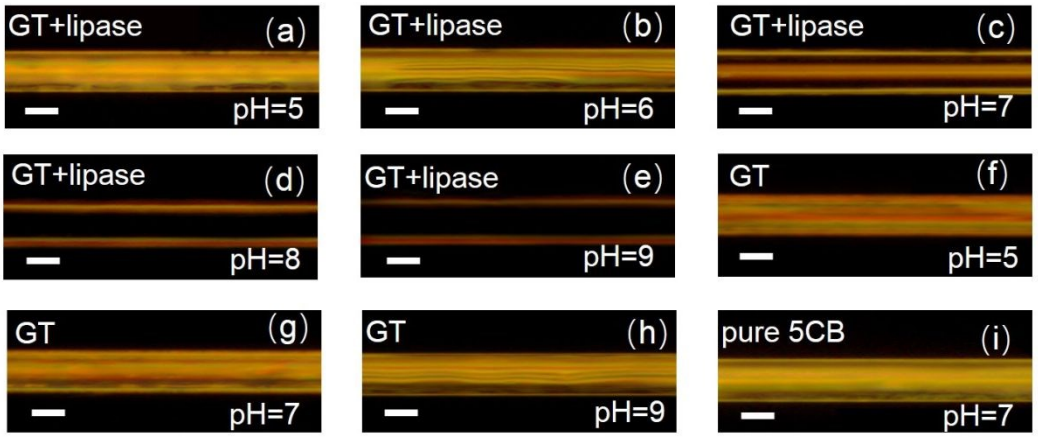


**Fig. 4.** Polarized optical microscope (POM) images of GT-doped 5CB microfibers with a diameter of 65 μm immersed in (a – e) 100 μg/mL lipase and (f – g) pure PBS with different pH. (i) POM images of pure 5CB microfibers immersed in 100 μg/mL lipase with pH=7. Scale bar: 50 μm.

PPEs is given. The nonlinear increase similar to the knee joint shows the lasing phenomenon. The nonlinear increase similar to the knee joint shows the lasing phenomenon. This indicates that the lasing emission may originate from WGMs, which is benefit of the cylindrical axisymmetric structure and the smooth interface of 5CB microfiber.

To further verify the mechanism of lasing emission, the free spectral ranges (FSRs) of 5CB microcavities with different sizes were studied. The measured FSR was inversely proportional to the microcavity diameter (Fig. 3b). This is plausible because FSR = $\lambda^2/(n_{eff}\pi D)$, where λ is the resonant wavelength and $n_{eff}$ is the effective refractive index of the WGM microcavity [39,40]. In our experiments, the 5CB microfibers were immersed in distilled water to align the 5CB molecules parallel to the surface of the microfibers. Therefore, the effective refractive index of the WGM microcavity is the ordinary refractive index ($n_o$ = 1.54) of 5CB. As shown in the inset of Fig. 3b, the FSR of microfiber with diameters of 33 and 56 μm were 3.5 and 1.4 nm, respectively. Considering that the resonance wavelength λ is about 620 nm, the theoretical results are in good agreement with the experimental observations, which further verifies the WGM mechanism.

### 3.2 *The feasibility of GT-doped 5CB microfiber to detect lipase*

Lipase catalyzes the hydrolysis of GT to produce oleic acid. In addition, studies have found that at higher pH values, oleic acid molecules will be deprotonated to form amphiphilic surfactants [41]. Once the areal density of the amphiphile exceeds the critical value, the 5CB molecules will be induced to change from planar to homeotropic anchoring. Therefore, inspired by the above studies, we first investigated the feasibility of using GT-doped 5CB microfibers to detect lipase at a concentration of 100 μg/mL.

GT-doped 5CB microfibers with a diameter of 65 μm were immersed in lipase aqueous solutions (100 μg/mL) of different pH and pre-incubated for half an hour. When the pH of the solution was low (pH < 7), we did not observe an optical response of the 5CB microfibers, which showed a bright appearance (Figs. 4a and 4b) and was similar to the optical response of pure 5CB microfiber immersed in PBS solution (Fig. 4i). These results indicated that the 5CB molecules showed a planar anchoring at the LC/aqueous solution interface. However, when the pH of the solution was higher than 7, the appearance of the microfiber transition from bright to dark (Figs. 4c-4e). The reason is that higher pH promotes the deprotonation of oleic acid released by enzymatic hydrolysis, inducing a change in the anchoring state of 5CB from planar to homeotropic. Furthermore, we performed three additional controls in PBS without lipase to confirm that the optical response of the 5CB microfiber was caused by the enzymatic reaction between lipase and GT in the aqueous phase (Figs. 4f-4h).

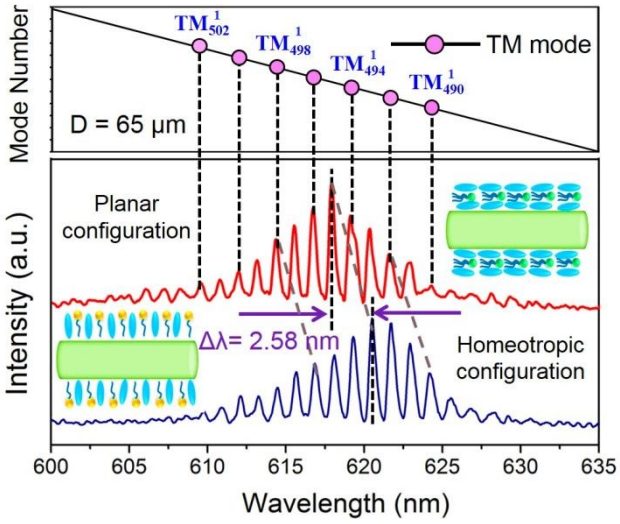


**Fig. 5.** WGM lasing of GT-doped 5CB microfibers with planar (red line) and homeotropic (blue line) configurations (bottom panel) and matching between the experimental observation of WGM lasing wavelengths and the calculated

lasing mode numbers (top panel). The GT-doped 5CB microfiber was placed in a lipase solution at a concentration of 100 μg/mL.

For a more accurate and reliable interpretation, we next examined the WGM spectral response as a quantitative description of the reaction process. The typical WGM spectrum

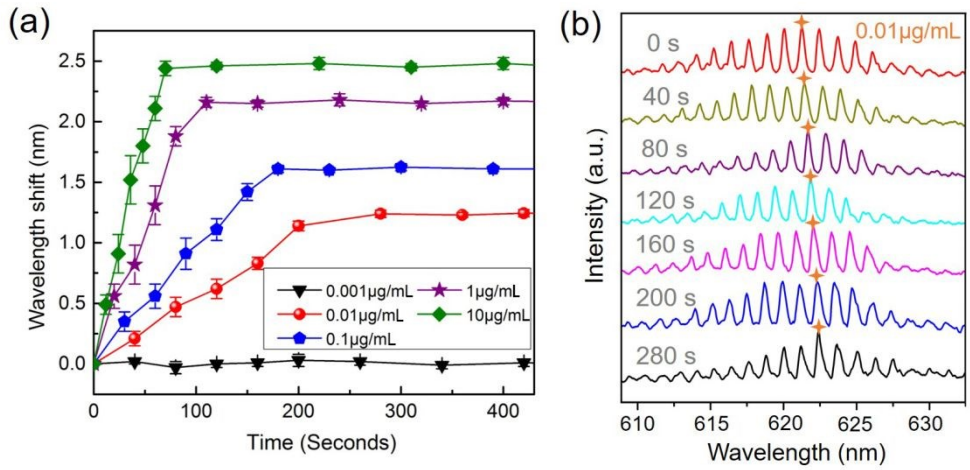


**Fig. 6.** (a) WGM wavelength shift with varying lipase concentrations. (b) Portion of WGM lasing spectra as a function of time. Spectra were collected from a 65-μm-diameter GT-doped 5CB microfiber in 0.01μg/mL lipase at pH=8.

of GT-doped 5CB microfiber under the excitation of the pump light is shown in Fig. 5 and the mode number of WGM was analyzed by using the theoretical asymptotic formulas as reported previously [39,42]. GT-doped 5CB microfiber was placed in a lipase solution at a concentration of 100 μg/mL. The red spectrum line was recorded at the initial stage of hydrolysis, at which 5CB molecules were arranged parallel to the fiber surface. During the reaction, 5CB molecules gradually changed from planar to homeotropic anchoring and the WGM spectrum of the microfiber produced a significant redshift response. The obtained homeotropic configuration resulted in a wavelength shift of 2.58 nm, as shown in Fig. 5. These results indicated indicates that the spectral shift caused by the structural change of the 5CB microfiber demonstrates the capability of quantified quantifying the enzymatic reaction between lipases and GT.

### *3.3 Sensitivity for lipase detection*

The concentration-dependence of the WGM wavelength shift was next investigated by changing the concentration of the lipase solution. Considering the deprotonation conditions of oleic acid and the optimal pH of lipase, the PBS solution with pH value of 8 was selected as the lipase detection medium. In the detection, we determine the minimum lipase concentration that the sensor can respond to as the detection limit. A 100 μg/mL lipase solution was serially diluted 10, 100, 1000, 10000, and 100000 folds for testing. The different responses of the proposed WGM lasing-based LC sensor to different concentrations of lipase are shown in Fig. 6a and Table S1. In the presence of 10 μg/mL lipase, the sensing system had a rapid initial response and the wavelength shift reached saturation within 80 seconds. However, for a concentration of 0.1 μg/mL, the equilibration time was about twice that of the former, and the saturation level was lower. A similar trend was found with further reductions in lipase concentrations. We found that the minimum lipase concentration that the sensor can detect is 0.01 μg/mL. At this concentration, the wavelength shift of WGM is ~1.22 nm within 200 seconds. At the lowest concentration used (0.001 μg/ml), no significant WGM spectral response was observed above the noise level within a monitoring window of up to 420 seconds. Therefore, the detection limit of the proposed WGM lasing-based LC sensor for lipase was determined to be 0.01 μg/ml.

View Article Online
DOI: 10.1039/D0AN01187H

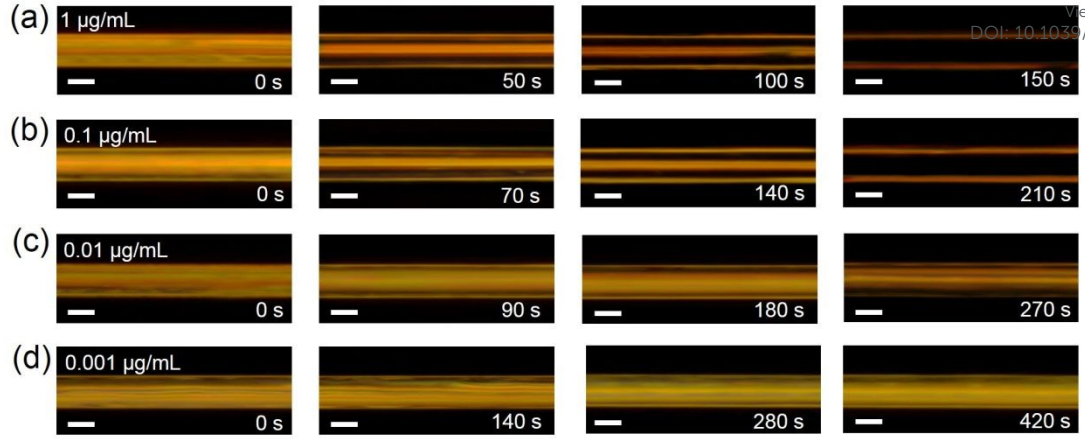


**Fig. 7.** Evolution of POM images of 65-μm-diameter GT-doped 5CB microfiber in (a) 1 μg/mL, (b) 0.1 μg/mL, (c) 0.01 μg/mL, (d) 0.001 μg/mL lipase at pH = 8. Scale bar 50 μm.

In addition, based on the results of Fig. 6a and Table S1, a fitting curve of lipase with different concentrations and WGM wavelength shift was obtained, as shown in Fig. S2 in Supplementary information. All these results demonstrate the ability of the proposed WGM lasing-based LC sensor to detect lipase effectively.

Finally, we compared our detection method with conventional LCs optical appearance detection method. A similar experimental procedure was performed again, and the appearance of the 5CB microfiber was used to the sensing signals. The time-dependent polarized patterns of the microfiber with different lipase concentrations are summarized in Fig. 7.

When the lipase concentration was 1 μg/mL or 0.1 μg/mL, the black appearance of 5CB microfiber was visible. However, with the further decrease of lipase concentration, the bright-to-dark appearance was no longer obvious. In particular, at the lipase concentration was as low as 0.01 μg/mL, the appearance response was quite weak and difficult to judge with the naked eye. It is worth noting that, at the same lipase concentration, we observed a considerable and quantitative wavelength shift of WGMs. Therefore, these results showed the potential superiority of our WGM-based 5CB microfiber biosensor for biochemical detection and could be an effective alternative to conventional detection methods based on LC materials.

***3.4 Selectivity for lipase detection***

The comparison between the proposed WGM lasing-LC sensor and other methods is shown in Table 1. The detection sensitivity of the proposed sensor is comparable to that of colorimetric and chromatographic methods. However, compared with fluorimetric assay and enzyme immunoassay, the sensitivity of the proposed sensor is still relatively low. It is worth mentioning that our detection limit is optimal in the reported LC material-based lipase detection methods. Even compared with the traditional detection methods, the proposed sensor has a certain advantage in detection range and detection time.

Further improving the detection sensitivity of the sensor is the focus of our future work. In the sensor based on the WGMs, the Q-factor of the microresonator is positively correlated with the detection sensitivity of the sensor[15]. For an optical microcavity, one of the effective ways to enhance its Q-factor is to reduce the scattering loss of circulating light in the cavity by appropriately increasing the radius of curvature of the microresonator[15]. Therefore, in the next work, we will improve the manufacturing process, try to increase the diameter of the cylindrical LC microfiber, improve the Q-factor of the microresonator, and enhance the sensitivity of the sensor. We also hope that through these improvements, the proposed sensor can meet the requirements for the detection of lipase in human blood.

View Article Online
DOI: 10.1039/D0AN01187H

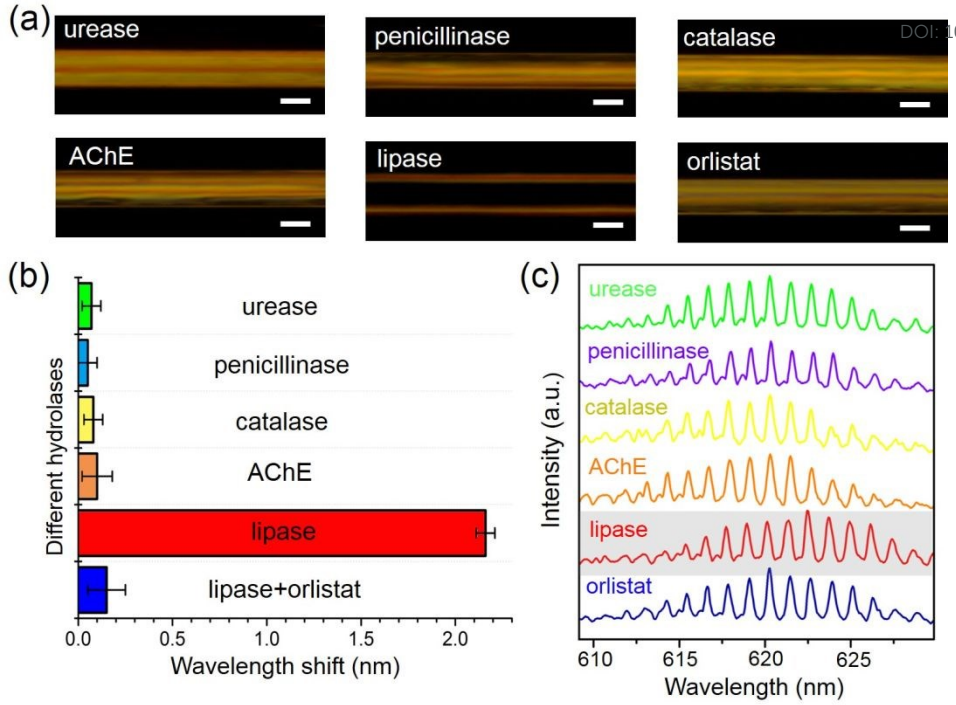


**Fig. 8.** POM images of 65-μm-diameter GT-doped 5CB microfiber in 1 μg/mL of urease, penicillinase, catalase, AChE, lipase, and orlistat (a lipase inhibitor), respectively. Scale bar 50 μm. (b) Comparison of WGM wavelength shifts for lipase and other hydrolytic enzymes or inhibitor. (c) WGM lasing spectra of GT-doped 5CB microfiber in different reaction solutions.

**Table 1. Comparison of different methods for lipase detection**

| Detection Method | Sensing Structure | Detection Range | Detection Limit | Detection time | References |
|---|---|---|---|---|---|
| Chromatographic assay | —— | 0.1 – 16 μg/mL | 0.15 μg/mL | 120 min | [43] |
| Enzyme immunoassay | —— | 0.5 – 100 ng /mL | 0.5 ng /mL | —— | [29] |
| Fluorimetric assay | —— | 0.1 – 3 ng/mL | 0.1 ng/mL | —— | [44] |
| Fluorimetric assay | —— | 0.05 - 1 μg /mL | 0.05 μg /mL | 160 min | [45] |
| Colorimetric Assay | —— | 0.01 – 10 μg/mL | 0.01 μg/mL | —— | [46] |
| Colorimetric assay | —— | 0.5 – 2 μg/mL | 0.5 μg/mL | 15 min | [47] |
| Optical pattern-based LC sensor | Planar | 1 – 100 μg/mL | 1 μg/mL | 3 h | [48] |
| Optical pattern-based LC sensor | Spherical | 1 – 100 μg/mL | 1 μg/mL | 2 h | [41] |
| Optical pattern-based LC sensor | Hemispheric | 0.1 – 10 μg/mL | 0.1 μg/mL | 6 min | [49] |
| WGM lasing-based LC sensor | Cylindrical | 0.01– 100 μg/mL | 0.01 μg /mL | ＜200 s | Present work |

In addition to high sensitivity, the selectivity for the detection target is another important factor of the biosensor. Since biosensors often need to be applied in complex and diverse environments, the ability to avoid interference of other molecules is a crucial attribute.

We tested five different hydrolases at the same concentration of 1 μg/mL, including lipase, urease, penicillinase, AChE, and catalase. For accuracy, the detection was carried out with the detection of both LC polarized patterns and WGM spectral responses. All experiments were performed three times and the results can be repeatable. As shown in Fig. 8a, except for lipase, all the other four hydrolases showed a bright appearance, indicating that no hydrolysis reaction occurs during the detection process. Furthermore, these similar results are more quantitatively and effectively characterized by WGM wavelength shift, as shown in Figs. 8b and 8c. We found the proposed biosensor was much more responsive to lipase than the other four hydrolases. The reason is that the GT we doped is an unsaturated glyceride, and lipase has a highly efficient hydrolysis efficiency on it, while other types of hydrolases have much lower hydrolysis ability than lipase.

Moreover, to further confirm the spectral response was from lipase, we added the inhibitor orlistat (1 μg/mL) to the lipase solution. The same experimental procedure was performed again, but we did not detect any significant spectral shift signal. Therefore, the WGM-based 5CB microfiber biosensor is highly selective for lipase. In addition, the enzyme inhibition experiment also provides new insights into the detection of lipase inhibitors.

## 4. Conclusions

In summary, we have developed a 5CB microfiber biosensor based on WGM for real-time, quantitative, and sensitive monitoring of lipase concentration. The sensor structure of active soft-matter resonator was adopted, and the lasing signal was collected by a free-space optical device. Due to direct physical contact with the microresonator is avoided, the mechanical stability of the entire sensing system can be significantly enhanced. In addition, we can also expect to combine this WGM sensing device with microfluidic technology to obtain better sensing performance and produce a real-time online detection platform that meets the practical application requirements.

The wavelength shift of the WGM spectrum can be used as an effective indicator of lipase concentration. The detection limit of lipase was as low as 0.01 μg/mL within 200 seconds. Also, the sensing system is highly selective for lipase, which can effectively avoid the interference of foreign biochemical molecules. These results indicate that the proposed WGM-based 5CB microfiber biosensor has great potential for quantitative and sensitive detection of biochemical interactions.

However, so far, we have not found a way to recycle the proposed microfiber biosensor. Therefore, the LC microfibers are for single-use application at present. Fortunately, the preparation of microfibers is relatively simple and does not require complex manufacturing equipment. This makes LC microfibers with the potential to be prepared in large quantities, and to a certain extent can make up for the shortcomings of the single applications.

## Conflicts of interest

There are no conflicts to declare.

## Acknowledgements

This work was supported by the National Natural Science Foundation of China (No. 61975040), the Fundamental Research Funds for the Central Universities (No. 3072020CF2514) and the PhD Student Research and Innovation Fund of the Fundamental Research Funds for the Central Universities (No. 3072020GIP2520).

## Notes and references

1 R. J. Carlton, J. T. Hunter, D. S. Miller, R. Abbasi, P. C. Mushenheim, L. N. Tan and N. L. Abbott, *Liq. Cryst. Rev.*, 2013, **1**, 29–51.
2 D. S. Miller, X. Wang and N. L. Abbott, *Chem. Mater.*, 2014, **26**, 496–506.
3 M. I. Kinsinger, B. Sun, N. L. Abbott, and D. M. Lynn, *Adv. Mater.*, 2007, **19**, 4208–4212.
4 J. Y. Du, Q. F. Jiang, X. C. Lu, L. C. Chen, Y. Zhang and X. L. Xiong, *Analyst*, 2019,**144**, 1761-1767
5 M. I. Kinsinger, M. E. Buck, N. L. Abbot and D. M. Lynn, *Langmuir*, 2010, **26**, 10234–10242.
6 Y. Y. Luk, M. L. Tingey, K. A. Dickson, R. T. Raines and N. L. Abbott, *J. Am. Chem. Soc.*, 2004, **126**, 9024–9032.
7 C. Xia, D. Zhou, Y. Su, G.Zhou, L, Yao, W. Sun and Y. Liu, *Analyst*, 2020, Advance Article.
8 X. Bi, D. Hartono and K.-L. Yang, *Adv. Funct. Mater.*, 2009, **19**, 3760–3765.
9 A. D. Price and D. K. Schwartz, *J. Am. Chem. Soc.*, 2008, **130**, 8188–8194.
10 K. J. Vahala, *Nature*, 2003, **424**, 839–846.
11 M. Humar, M. Ravnik, S. Pajk and I. Musevic, *Nat. Photonics*, 2009**, 3**, 595–600.
12 A. Bozzola, S. Perotto and F. De. Angelis, *Analyst*, 2017, **142**, 883-898.
13 Y. Wang, H. Li, L. Zhao, Y. Liu, S. Liu and J. Yang, *Opt. Express*, 2017, **25**, 918–926.
14 V. S. Ilchenko and A. B. Matsko, I*EEE J. Sel. Top. Quantum Electron.*, 2006, **12**, 15–32.
15 G. Righini, Y. Dumeige, P. Féron, M. Ferrari, G. Nunzi Conti, D. Ristic, and S. Soria, *Riv. Nuovo Cim.*, 2011, **34**, 435–488.
16 H. Li, B. Sun, Y. Yuan and Y. Yang, *Opt. Express*, 2019, **27**, 1991–2000.
17 M. Humar and I. Muševič, *Opt. Express*, 2011, **19**, 19836–19844.
18 F. Vollmer, S. Arnold and D. Keng, *PNAS*, 2008, **105**, 20701-20704.
19 A.L. Washburn, M.S. Luchansky, A.L. Bowman and R.C. Bailey, *Anal. Chem.*, 2009, **82**, 69-72.
20 R. Duan, X. Hao, Y. Li and H. Li, *Sens Actuators B.*, 2020, **308**,127672.
21 X. D. Fan, J. D. Sutter, I. M. White, H. Y. Zhu, H. D. Shi and C. W. Caldwell, *Biosens. Bioelectron.*, 2008, **23**, 1003–1009.
22 F. C. Wu, Y. Wu, Z. Niu and F. Vollmer, *Analyst*, 2015,**140**, 2969-2972.
23 A. M. Armani, R. P. Kulkarni, S. E. Fraser, R. C. Flagan and K. J. Vahala, *Science*, 2007, **317**, 783–787.
24 F. Vollmer and S. Arnold, *Nat. Methods*, 2008, **5**, 591–596.
25 P. Reis, K. Holmberg, H. Watzke, M.E. Leser and R. Miller, *Adv. Colloid Interface Sci.*, 2009, **147**, 237-250.
26 P.R. Solanki, C. Dhand, A. Kaushik, A.A. Ansari, K.N. Sood and B.D. Malhotra, *Sens Actuators B.*, 2009, **141**, 551–556.
27 A. Houde, A. Kademi and D. Leblanc, *Appl. Biochem. Biotechnol.*, 2004, **118**,155-170.
28 R. Singh, N. Gupta, V.K. Goswami and R. Gupta, *Appl. Microbiol. Biotechnol.*, 2009, **70**, 679–682.
29 J. Carrére, C. Galabert, J. P. Thouvenot and C. Figarella, *Clin. Chim. Acta*, 1986, **161**, 209-219.
30 G.B. Mills, W.H. Moolenaar, *Nat. Rev. Cancer*, 2003, **3**, 582–591.
31 F. Beisson, A. Tiss, C. Rivière and R. Verger, *Eur. J. Lip. Sci. Technol.*, 2000, **102**, 133-153.
32 F. Hasan, A.A. Shah and A. Hameed, *Biotechnol. Adv.*, 2009, **27**, 782-798.
33 H.Li, X. Sun, M.K. Shahzad, and L. Liu, *J. Mater. Chem. C*, 2019,**7**, 7984-7992.
34 R. Duan, Y. Li, H. Li and J. Yang, *Talanta*, 2020, **209**, 120513.
*35* R. Duan, Y. Li, H. Li and J. Yang, *Biomed. Opt. Express*, 2019, **10**, 6073–6083.

View Article Online
DOI: 10.1039/D0AN01187H

36 P. D. I. Fletcher, N. G. Kang and V. N. Paunov, *ChemPhysChem*, 2009, **10**, 3046 – 3053.
37 J. Kurniawan, K. Suga and T.L. Kuhl, *Bba-Biomembranes*, 2017, **1859**, 211–217.
38 Q. Lu, X. Chen, L. Fu, S. Xie and X. Wu, *Nanomaterials*, 2019, **9**, 479.
39 V.D. Ta, R. Chen, L. Ma, Y.J. Ying and H.D. Sun. *Laser Photon Rev*, 2013, **7**, 133–139.
40 R. Chen, V. D. Ta and H. D. Sun, *ACS Photonics*, 2014, **1**, 11–16.
41 Q.Z. Hu and C.H. Jang, *Analyst*, 2012, **137**, 5204–5207.
42 C. C. Lam, P. T. Leung and K. Young, *J. Opt. Soc. Am. B*, 1992, **9**, 1585 −1592.
43 V. Maurich, M. Moneghini, M. Zacchigna, A. Pitotti and E. Lencioni, *J. Pharm. Biomed. Anal.*, 1991, **9**, 427-431.
44 F. Beisson, N. Ferté, J. Nari, G. Noat and R. Verger, *J. Lipid Res.*, 1999, **40**, 2313-2321.
45 J. -F. Jette, and E. Ziomek, *Anal. Biochem.* 1994, **219**, 256-260.
46 S. J. Choi, J. M. Hwang and S. I. Kim, *J. Biochem. Mol. Biol*., 2003, **36**, 417-420.
47 R. Singh, N. Gupta, V. K. Goswami and R. Gupta, *Appl. Microbiol. Biotechnol.*, 2006, **70**, 679-682.
48 Q.Z. Hu and C.H. Jang, *Talanta*, 2012, **99**, 36-39.
49 Q.Z. Hu and C.H. Jang, *Liq. Crys.*, 2014, **41**, 597-602.

View Article Online
DOI: 10.1039/D0AN01187H

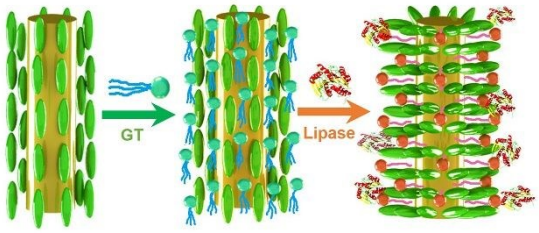


We demonstrate a quantitative and sensitive strategy for monitoring lipase concentration using a liquid crystal microfiber biosensor based on whispering-gallery mode.